# CHAPTER-5

# Revolutionizing Agriculture with Nanotechnology: Rice-Based Silica Nanoparticles for the Remediation and Quantification of Toxic Heavy Metals in Potatoes

## 5.1: INTRODUCTION

The presence of toxic heavy metals in food products is becoming an increasing source of worry due to the possible dangers they pose to human health. Potatoes, a crop that's used in a lot of different dishes, can be dangerous to eat if they're contaminated with toxic heavy metals. To ensure food safety and protect public health, it is crucial to evaluate the levels of toxic heavy metals in potatoes and take corrective action as needed. [1]. This study work focuses on the measurement of toxic heavy metals in potatoes from the North Gujarat region known as "KURFI BADSHAH" and investigates the usage of SNPs synthesised from GNR-3-SNPs as a biomass adsorbent for the purpose of food product remediation using silica nanoparticles as a biomass adsorbent. Trace amounts of toxic heavy metals like Co, Ni, Pb, Cd, and Cr can enter the food chain from a number of different places [2]. These places include the soil, the water, and agricultural inputs.

Toxic Heavy metals can accumulate in plants, especially potatoes, when they are absorbed by plants growing in contaminated soil or water. Regular consumption of tainted potatoes can lead to serious health issues down the road, such as organ damage, neurological illnesses, and even cancer [3]. Therefore, it is extremely necessary to monitor and quantify the concentrations of toxic heavy metals in potatoes in order to evaluate the potential for harm to the health of consumers.

ICP-MS was used to analyse potato samples for heavy metal concentrations for this study. ICP-MS is a technology for identifying trace elements that is both very sensitive and accurate. Therefore, the concentration of toxic heavy metals in dietary samples may be determined with high accuracy [4].

To address the issue of toxic heavy metal contamination in potatoes, we looked at the use of SNPs synthesised from RHA as a potential remediation strategy. Rich in silica, RHA is a by-product of the agricultural industry. SNPs can be synthesised from RHA, synthesis of SNPs adsorbents environmentally friendly and cost-effective.

20% of a rice grain's total weight is made up of its husk (RH) [5]. It's a by-product of the rice industry, something that happens naturally as a result of doing business. Since RH landfills are frequently set on fire, open burning has surpassed other methods as the most popular way to dispose of RH garbage [6,]. For more than 3 billion people, rice is the primary source of

nutrition, but rice cultivation generates a lot of agricultural waste [7,8]. Straw, husk, and ash are all examples of what are considered garbage. More than 120 metric tonnes of RH are expected to be wasted annually after grinding is complete [9]. In order to obtain high-quality rice kernels for human consumption, rice milling is required; as a result, waste management must adhere to the concepts of sustainable agriculture and the circular economy [10]. In this research, we used a strain of rice local to the Navsari area, which we've dubbed "GNR-3." Which is already presented in Characterization of the synthesised SNPs was performed using a number of different approaches in order to assess their potential for use in the removal of toxic heavy metals. TGA was performed to ascertain the SNPs' thermal stability. The XRD analysis provided insight into the SNPs crystal structure and phase composition. SEM and TEM were used to examine the SNPs shape, size, and surface characteristics. To determine the chemical composition of the SNPs, EDX was used. The specific surface area of the SNPs was determined by BET analysis, and the SNPs topography was thoroughly evaluated via AFM.

The use of SNPs produced in the Navsari area "GNR-6" for the remediation of food products is a novel approach to the problem of heavy metal contamination in agricultural output. This approach was developed by combining the toxic heavy metal quantification in North Gujarat area "Kufri Badshah" potatoes with the use of SNPs produced in the Navsari region. This investigation is being carried out with the goal of making a contribution to the development of procedures that are efficient and sustainable for ensuring the quality and safety of food products.

## 5.2: RESULTS AND DISCUSSION

### 5.2.1: Characterization of SNPs

### 5.2.1.1: FT IR

Figure 2 shows that the FT IR spectra of the SNPs samples exhibit a number of characteristic bands that are associated with specific vibrations and functional groups. The band at 3457.05 $cm^{-1}$ is caused by the stretching vibration of the O-H group. This is evidence that the samples under study include hydroxyl groups (O-H). The band at 1649.57 $cm^{-1}$ seen in both SNPs samples was traced back to the bending vibration of $H_2O$ molecules in the Si-OH group. This leads one to conclude that there are water molecules present that are associated with the

silanol (Si-OH) groups. Bands can be seen at 1083.29 cm$^{-1}$ because of an asymmetric stretching vibration in the Si-O-Si bonds. This proves that silicon, oxygen, and silicon linkages are present in the samples. An exceptionally noticeable peak can be noticed at 795.48 cm$^{-1}$, and its origin may be traced back to the stretching vibration of symmetric Si-O bonds. This is evidence that the silica network contains silicon-oxygen bonds (Si-O bonds). The bands at 463.46 cm$^{-1}$ correspond to vibrations in the siloxane groups present in the SNPs samples, and the Si-O bond is bent as a result. This is indicative of the presence of bent silicon atoms bonded to oxygen atoms. The results show that silanol groups (Si-OH) are formed when sodium silicate is dissolved in HCL, and siloxane groups are formed when sodium silicate is subjected to condensation. The information presented here provides a deeper understanding of the structural alterations and functional group modifications that take place during the therapy process (Table 1) [11, 12].

**Table 1:** Data from an FT IR spectrometer on SNPs that were synthesised from GNR-3 rice

| Wavenumber (cm$^{-1}$) | Functional Group/ Vibration | Assignment |
| --- | --- | --- |
| 3457.05 | O-H Stretching | Stretching vibration O-H group |
| 1649.57 | | Bending vibration of $H_2O$ molecule in the Si-OH group |
| 1083.29 | Si-O-Si Asymmetric Stretching | Asymmetric stretching vibration of Si-O-Si |
| 795.48 | Si-O Symmetric Stretching | Symmetric stretching vibration of Si-O bond |
| 463.46 | Si-O Bending (siloxane group) | Si-O bending of siloxane group |

For a better grasp of the SNPs chemical structure and properties, the FT IR analysis provides useful information regarding their composition and bonding characteristics. [13-19].
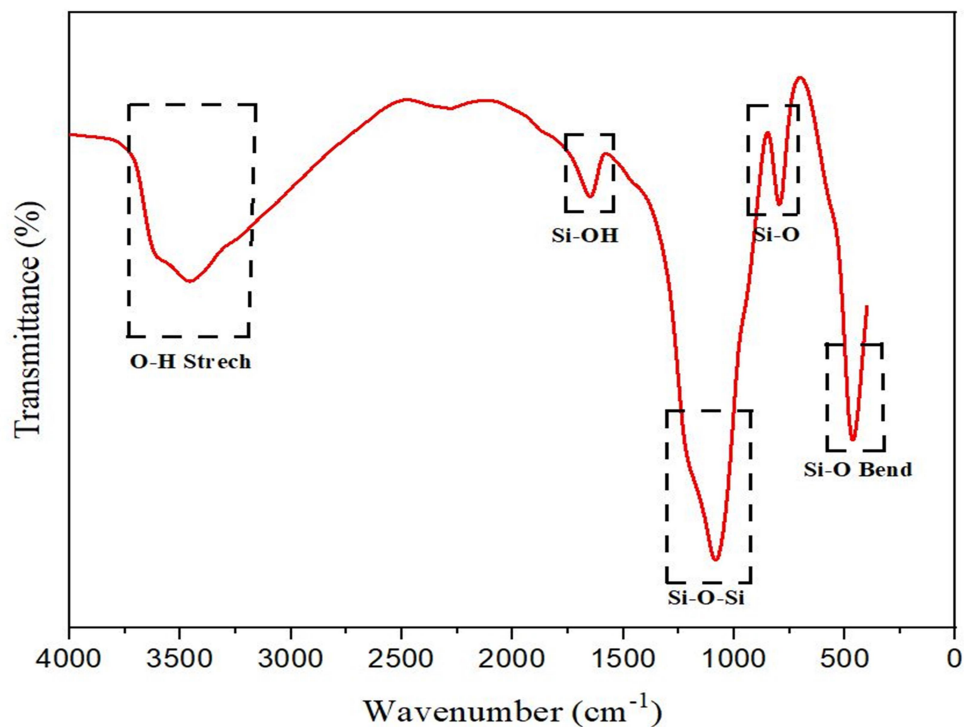
**Fig. 2:** Analysis of SNPs produced from GNR-3 rice husk using FT IR

## 5.2.1.2: SEM

SEM analysis of high-quality SNPs extracted from RHA (particle sizes: 20-80 nm) is depicted in Figure 2. SNPs are the best absorbent for getting rid of toxic heavy metals because of their high adsorption capacity.
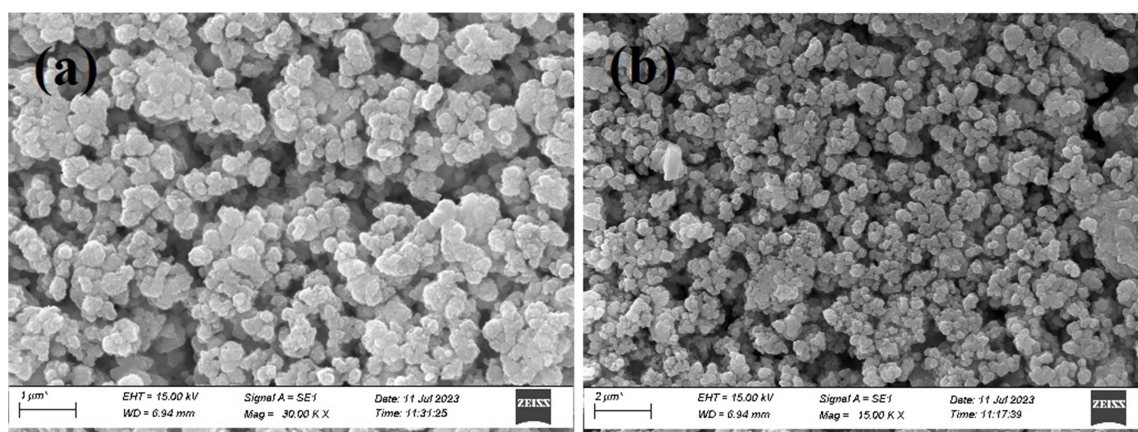


**Fig. 2:** An examination of SNPs using the SEM at varying levels of magnification and scale

### 5.2.1.3: EDX

The EDX analysis proved that the SNPs isolated from the RH were pure. The outcomes of EDX on the SNPs are shown in Figure 3. The region of interest in the SEM image used for EDX analysis is highlighted in Figure a. As can be seen in Figure (b), the spectra showed distinct signal peaks for Si (45.36%), O (37.5 %), Na (9.5 %), and Au (7.1 %). The EDX spectra, which demonstrated that the observed peaks matched those of oxygen and silica, provided conclusive evidence that the SNPs that were generated were composed of silica. Because of this outcome, it is clear that the SNPs sample was accurate. In addition, the investigation revealed the presence of a gold coating, which is evidence that (Au) was present in the results [24].
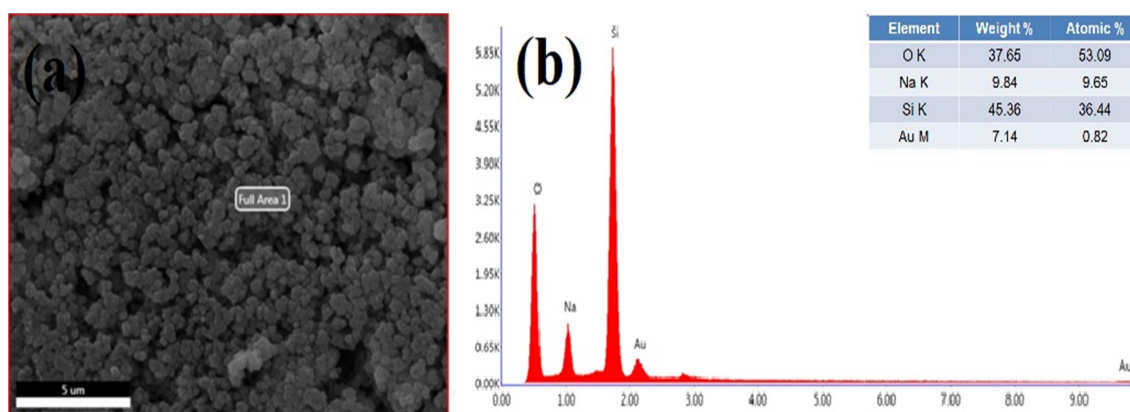


| Element | Weight % | Atomic % |
|---------|----------|----------|
| O K | 37.65 | 53.09 |
| Na K | 9.84 | 9.65 |
| Si K | 45.36 | 36.44 |
| Au M | 7.14 | 0.82 |

**Fig. 3:** (a) SEM picture of single nucleotide polymorphisms (b) EDAX spectrum of SNPs

### 5.2.1.4: PSD

This study presents a thorough particle size characterization of high-quality SNPs synthesised from RHA with a dynamic diameter range between 200 and 500 nm, evaluated using DLS in aqueous dispersion (Fig. 4). The SNPs have a dynamic diameter range between 200 and 500 nm. The PSA conclusions showing the size distributions are well-dispersed and under control are corroborated by the SEM research. This is because the DLS approach is frequently used to estimate the dynamic dimension particle sizes of SNPs dispersed in water. This is the reason why this is the case. The picture's results further indicated that the particle size distribution of the SNPs is bell-shaped, which is another name for the Gaussian distribution [25-27].
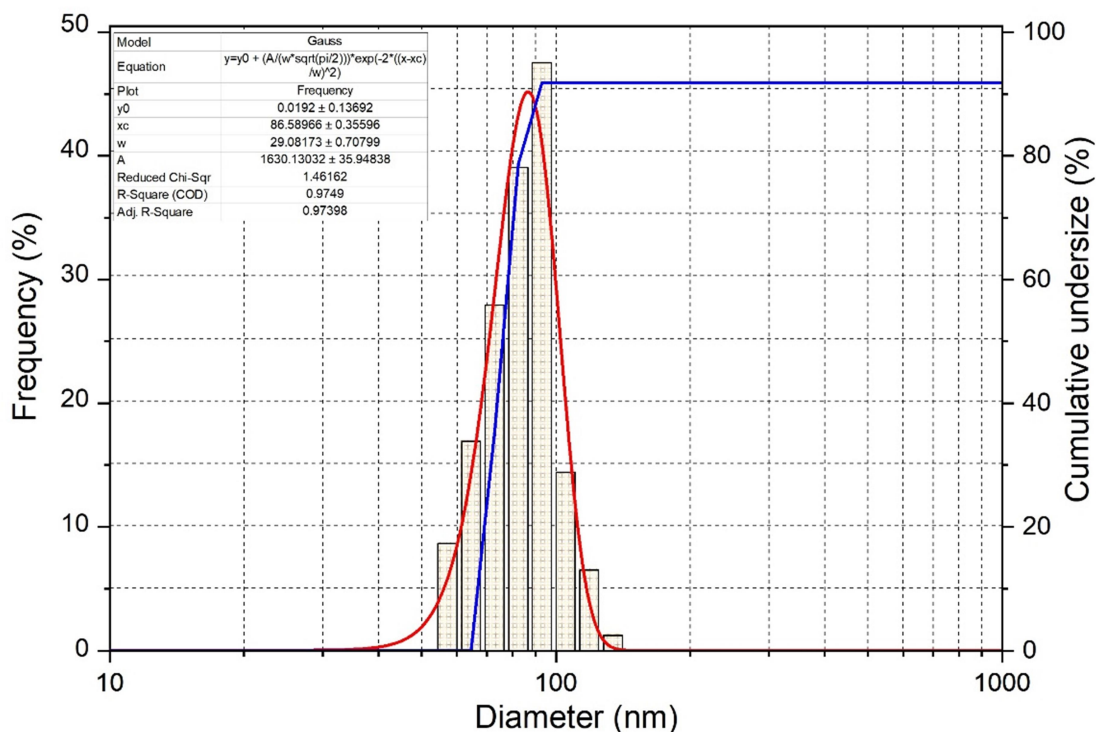
| Model | Gauss |
| Equation | y=y0 + (A/(w*sqrt(pi/2)))*exp(-2*((x-xc)/w)^2) |
| Plot | Frequency |
| y0 | 0.0192 ± 0.13692 |
| xc | 86.58966 ± 0.35596 |
| w | 29.08173 ± 0.70799 |
| A | 1630.13032 ± 35.94838 |
| Reduced Chi-Sqr | 1.46162 |
| R-Square (COD) | 0.9749 |
| Adj. R-Square | 0.97398 |

**Fig. 4:** Particle size analysis of SNPs

## 5.2.1.5: BET

The BET method, widely acknowledged for its accuracy in determining surface area, was employed to quantify the specific surface area of the SNPs. The obtained value of 11.1984 m²/g reflects the extent of surface available for adsorption. Concurrently, the pore size, a crucial factor influencing the accessibility of adsorption sites, was measured at 196.202 Å. The specific surface area of 11.1984 m²/g suggests a considerable active surface for potential interactions. This parameter is directly correlated with the adsorption capacity of the material, indicating a higher potential for accommodating adsorbate molecules. The synthesis process from rice husk appears to have effectively created a nanoparticle structure conducive to increased surface area. The observed pore size of 196.202 Å is notably large, and such macroscopic pores are known to enhance the accessibility of adsorption sites. Larger pores facilitate the diffusion of adsorbate molecules into the material, contributing to an improved adsorption capability. The synthesis method has evidently resulted in a nanoparticle structure characterized by a significant pore size, which is advantageous for applications requiring efficient adsorption. The combined effect of the substantial specific surface area and larger pore size is anticipated to yield a material with superior adsorption capability. The increased

surface area provides more active sites for adsorption, while the larger pores facilitate the swift ingress of adsorbate molecules into the internal structure. This synergistic combination enhances the overall adsorption performance of the SNPs [28-30].

## 3.2.1.6: TEM

In order to fully explore the characteristics of SNPs, TEM was used in this study. The investigation included measurements of the SNPs size, shape, uniformity, and homogeneity, which yielded extremely helpful information regarding the possible applications of these SNPs. Utilising the ImageJ software allowed for the generation of the size distribution histogram that can be found represented in Figure 5(b). This histogram was painstakingly created. This histogram does a good job of illustrating how the frequency distribution of different particle sizes looks. Notably, the distribution of the SNPs under consideration appears to follow a pattern that is rather usual, as indicated by the appearance of an almost log-normal curve in the histogram. The TEM study revealed that the SNPs predominantly display spherical morphology, which is related to both their size and shape. It was discovered that their sizes ranged anywhere from 20 to 50 nm. It was determined that a size of roughly 33.73 nm was the one that occurred most frequently within the population. This particular size is representative of a sizeable fraction of the SNPs contained inside the sample, which exemplifies the reproducibility and uniformity of the synthesis process. It is essential to make a note of the fact that agglomerates can be seen in the TEM images. This phenomenon can be explained by the natural interactions that occur between smaller particles, which are largely driven by electrostatic attraction or the forces of Van der Waals. The overall significance of the findings is not diminished in any way by these agglomerates, despite the fact that they are an unavoidable occurrence. In point of fact, they offer supplementary data regarding the inter particle interactions as well as the forces that govern the assembly of the SNPs. The favourable size of the SNPs is one of the most important implications that can be drawn from this TEM research. Their relatively small dimensions, which fall somewhere in the range of 20 to 50 nm, show significant promise for a variety of different applications. This size range is particularly well-suited for applications where regulated particle size is crucial, making it an excellent choice for those applications. Producing and putting these SNPs to use could potentially be beneficial to a wide variety of fields, from the medical field to the materials science industry [31-36].
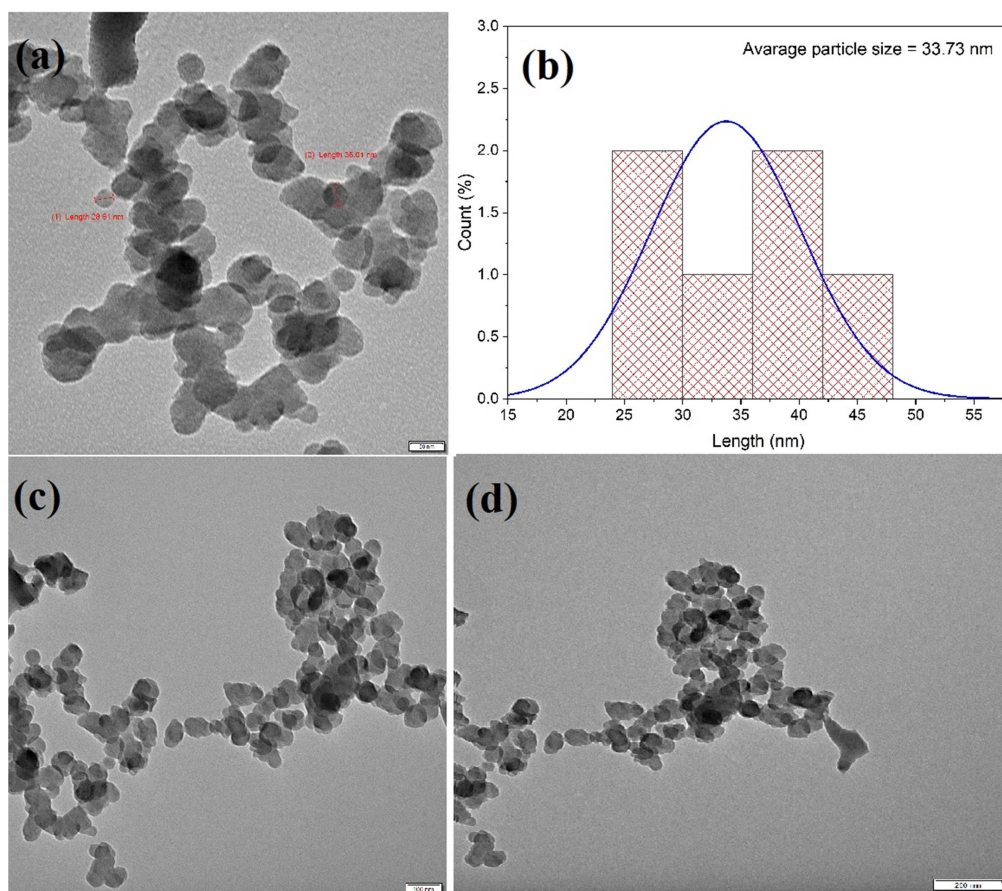
**Fig. 6:** TEM micrographs of single-nucleotide polymorphs (SNPs) (a) Scale of SNPs is 50 nm (b) Graph of the average particle size of SNPs (c) SNPs are measured on a scale of 100 nm. (d) The SNPs scale is 200 nm.

## 5.2.1.7: AFM

Images captured with an AFM reveal important details on the size, shape, and distribution of SNPs fabricated RHA. The AFM image, as shown in Figure 8(c), will most likely show a scattering of SNPs in the 20- to 50-nm size range. On the surface, these SNPs may have the impression of being small structures that are spherical or semi-spherical. Figure 8 (a), (b), and (d) are height profiles showing the Z-axis distance from the surface to the tip of the AFM probe. These height profiles may be seen in the figure. These profiles are going to correspond to changes in the height of the nanoparticles found throughout the sample. This image demonstrates how the SNPs are dispersed across the surface, despite the fact that there may be some size variation and clumping. Figure 9 is a representation of the surface contaminants

or pollutants, as well as the underlying structure of the rice husk ash, as seen by AFM pictures.
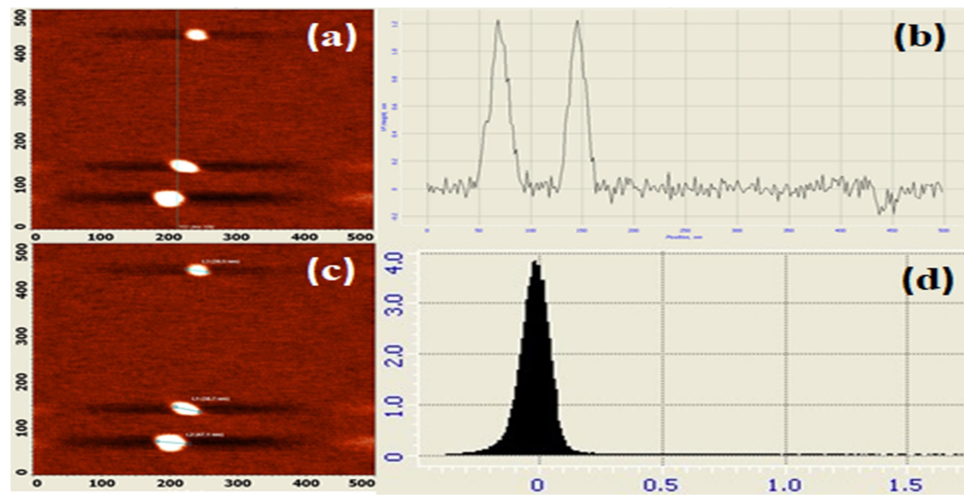


**Fig. 8:** Analysis by atomic force microscopy (AFM) of SNPs manufactured from GNR-3 rice husk (a) Particle height line (b) Particle height graph (c) Particle size (d) Particle size

It is possible that SNPs derived from rice husk ash will have a surface that is rough to some degree. Variations in the synthesis process or the inherent properties of the SNPs might be to blame for this roughness. Here we might notice clusters or agglomerations of SNPs in some sections of the image. This might suggest that the nanoparticles have a tendency to aggregate, which is something that occurs frequently in systems containing SNPs (Figure 9(e-l)). All of the images were captured at varying micrometres in order to analyse and analyse the surface topology as well as the roughness of the GNR-3 rice husk ash synthesised SNPs. [37-39].
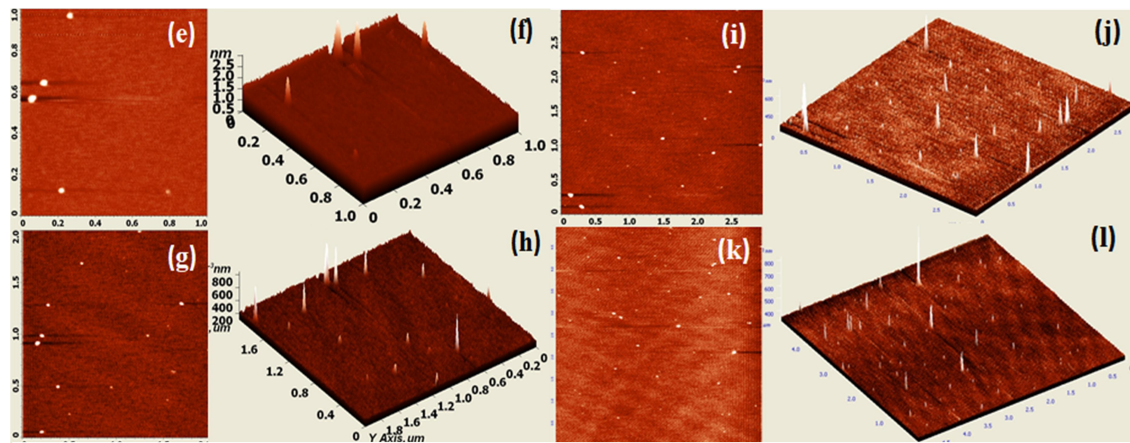


**Fig. 9:** AFM images of SNPs synthesized from GNR-3 rice husk (e) 1X1μm 2D (f) 1X1μm 3D (g) 2X2μm 2D (h) 2X2μm 3D (i) 3X3μm 2D (j) 3X3μm 3D (k) 5X5μm 2D (l) 5X5μm
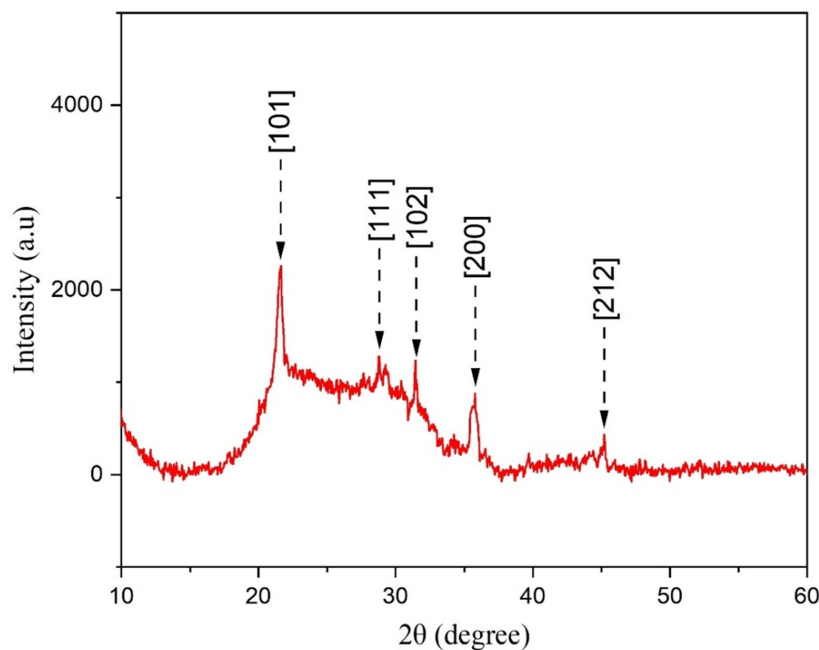
## 5.2.1.8: XRD



**Fig. 10:** XRD analysis of silica nanoparticles synthesized from GNR-3 rice husk

The XRD data show that there is a broad peak at 2 between 15° and 35°, confirming the presence of crystalline $SiO_2$, and a sharp peak at $2\theta = 22.1°$, confirming the presence of amorphous $SiO_2$. RH underwent thermal processing, which produced a heterogeneous mixture of crystalline and amorphous $SiO_2$ crystals. The presence of a prominent peak raises the possibility that tridymite structure was formed, which would point to crystalline $SiO_2$ being present. The intensity maxima at 28.82, 32.28, 36.83, and 46.12 degrees indicate that the amorphous phase was partially transformed into a crystalline silica structure. The $SiO_2$ analysis was compared to the silicon oxide $SiO_2$ powder diffraction file, which was located in the PDF#00-011-0695 folder. The principal diffracted peaks are shown by the arrows that are located in the diffractograms. At an angle of $2\theta = 22.01^0$, which coincided with the (101) plane, the most prominent peak was discovered. For $SiO_2$, numerous peaks disappeared at (111), (102), and (212), while others expanded and were less intense ((101), (200)). This was a sign that the silica's crystallinity was deteriorating. A nano scale substance can be identified by a broad peak that corresponds to the (101) plane; this broadening may be owing to scattering that is induced by SNPs. The possibility exists that this phase is amorphous $SiO_2$ since the amorphous broad peak is near to the primary peak of the (101) plane of $SiO_2$ crystalline [40-45].

## 5.3: TOXIC HEAVY METAL CONTAMINATION

Toxic Heavy Metals are a major cause for alarm because they can be both necessary and harmful components of certain organisms. The goal of this research was to examine the concentrations of many metals like Fe, Cu, Zn, Mn, Pb, Ni, and Cd in sixteen varieties of potatoes grown in Erzurum, Turkey. This study found that the "Kulfi Badshah" named potato cultivars analysed displayed a wide range of variation in the amounts of toxic heavy metals present. Fe > Zn > Mn > Cu > Ni > Pb > Cd is the accumulation order of metals in potato tubers. Food safety is very important, not only for the health of individuals but also for the health of society [46-48]. Some health concerns can be mitigated by eating a variety of foods, but the most significant supply of nutrients still comes from the staples. More than half of the world's population relies on rice as their primary source of nutrition; however the widespread cultivation of rice makes it more susceptible to contamination than other crops. For instance, rice has around a threefold greater tendency to collect toxic heavy metals than wheat [49,50]. There are risks to human health due to toxic heavy metals because of their toxicity, their accumulation in living organisms, and their potential for harmful effects. In an effort to lessen the severity of these health risks, a "maximum allowable concentration," or MAC, of heavy metals in rice has been determined by a consortium of international organisations and national governments. However, even concentrations of toxic heavy metals that are not quite as high as the MAC can be hazardous to human health. According to the findings of several studies, long-term exposure to arsenic at low levels might cause non-carcinogenic disorders such as cancer, hypertension, and neurological issues. In addition, the characteristics that determine exposure shift depending on age, body mass, and location, which increase the risks for populations that are already vulnerable. Because of this, health risk assessments need to take into account, in addition to MAC, other variables such as body weight, age, dietary preferences, and long-term intake (Table 2) [51,52].

**Table 2:** The impact of SNPs on the elimination of toxic heavy metals

| Replication | Adsorbent dose | Co (%) | Ni (%) | Pb (%) | Cr (%) |
|:---:|:---:|:---:|:---:|:---:|:---:|
| R-1 | 1:2 Potato | 1.9568 | 3.4132 | 0.8928 | 3.3378 |
| R-1 | 1:5 Potato | 0.7369 | 3.6617 | 0.4367 | 3.7117 |

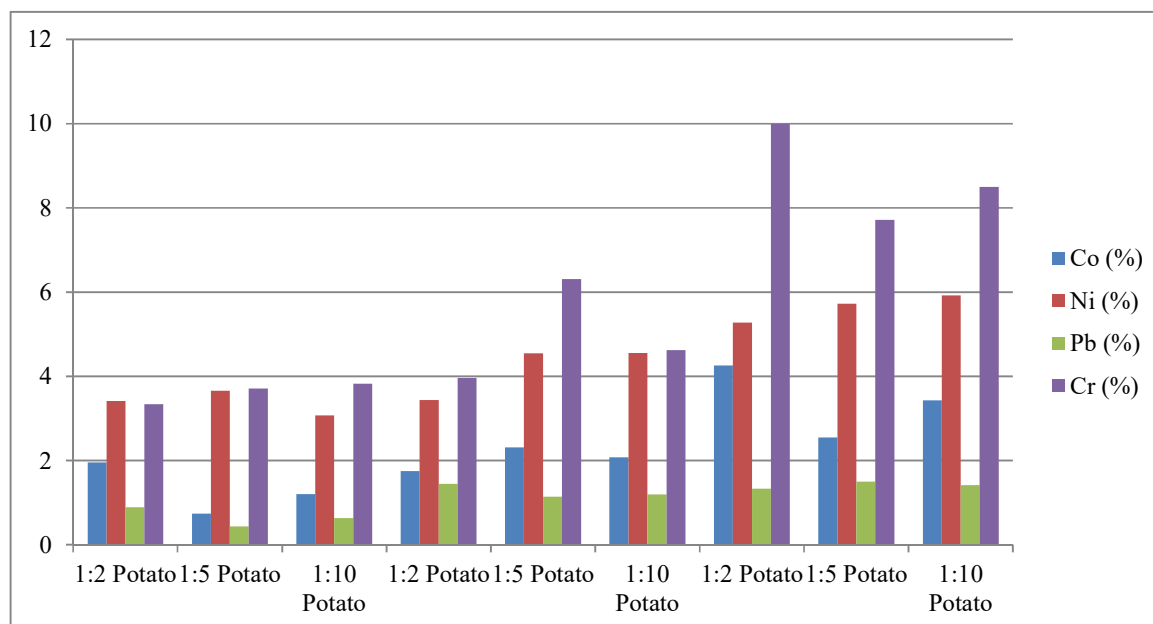| | | | | | |
|---|---|---|---|---|---|
| R-1 | 1:10 Potato | 1.2005 | 3.0718 | 0.6361 | 3.8194 |
| R-2 | 1:2 Potato | 1.7529 | 3.4398 | 1.4480 | 3.9646 |
| R-2 | 1:5 Potato | 2.3145 | 4.5475 | 1.1471 | 6.3093 |
| R-2 | 1:10 Potato | 2.0805 | 4.5591 | 1.1967 | 4.6195 |
| R-3 | 1:2 Potato | 4.2609 | 5.2824 | 1.3347 | 9.9880 |
| R-3 | 1:5 Potato | 2.5499 | 5.7236 | 1.4992 | 7.7131 |
| R-3 | 1:10 Potato | 3.4269 | 5.9233 | 1.4164 | 8.4979 |



**Figure 11:** Influence of Synthesized SNPs on the Removal of Toxic Heavy Metals

The data presented in Table 2 offers valuable insights into the impact of SNPs on the removal of harmful heavy metals, including Co, Ni, Pb, and Cr, using varying adsorbent doses in multiple replications. A key trend observed is that the effectiveness of SNPs in eliminating these toxic heavy metals is highly dependent on the chosen adsorbent dose. Generally, an increase in the adsorbent dose leads to better removal efficiency, which holds true for all four toxic heavy metals and is consistent across different replications (R-1, R-2, R-3). However, it's important to note that there are specific removal patterns for each heavy metal. For

example, Co removal efficiency varies between replications, with different adsorbent doses showing optimal results. Ni removal is most effective in Replication R-2 at a 1:5 Potato ratio, while in Replication R-3, the 1:10 ratio performs best. Pb removal shows that the 1:2 Potato ratio is consistently less efficient than the 1:5 and 1:10 ratios, while Cr removal efficiency generally favours the 1:5 and 1:10 Potato ratios. The data also underscores the variability across different replications (R-1, R-2, R-3), which may be attributed to various factors, including experimental conditions and the inherent diversity of toxic heavy metals behaviour in different environmental contexts. These findings have practical implications for environmental and health considerations, as they emphasize the importance of carefully selecting the appropriate adsorbent dose based on the target metal and the specific site conditions for effective toxic heavy metals removal.

Further research is essential to refine these findings, determine optimal adsorbent doses for various toxic heavy metals, and account for the variability observed in different replications. This data is a valuable contribution to the field of environmental science, offering guidance for future studies and practical strategies to address heavy metal contamination in environmental and industrial settings.

## 5.4: EFFECT OF BIOMASS CONCENTRATION ON METAL REMOVAL

The findings that were analysed and shown in Table 3 indicated that the use of SNPs in the group with ratios of 1:2 (SNPs: Potato), 1:5 (SNPs: Potato), and 1:10 (SNPs: Potato) successfully eliminated toxic heavy metal pollutants that were detected in biomass. Co removal (%) from potatoes using SNPs was found to be 1.298 0.62, 2.049 0.28, and 3.412 0.87 at the doses 1:2, 1:5, and 1:10 respectively after shaking for 6 h. Ni = 3.382 0.30, 4.182 0.64 and 5.643 0.33, Pb = 0.655 0.22, 1.264 0.16 and 1.417 0.08, and Cr = 3.623 0.25, 4.964 1.21 and 8. The ratio of SNPs to potatoes in the 1:10 (SNPs: Potato) and 1:2 (SNPs: Potato) treatments indicated a substantial difference in the elimination of toxic heavy metals. This suggests that the removal of potentially harmful toxic heavy metals from potatoes by SNPs is not affected by the quantity of potatoes present; the process continues regardless. This also suggests that the effectiveness of SNPs in eliminating toxic heavy metals from potatoes is substantial; even incremental increases in the quantity of potatoes boosted this efficiency.

**Table 3:** Elimination of high concentrations of toxic heavy metals

| Adsorbent dose | Co (%) | Ni(%) | Pb(%) | Cr(%) |
|---|---|---|---|---|
| 1:2 Potato | $1.298\pm0.62^b$ | $3.382\pm0.30^b$ | $0.655\pm0.22^b$ | $3.623\pm0.25^b$ |
| 1:5 Potato | $2.049\pm0.28^b$ | $4.182\pm0.64^b$ | $1.264\pm0.16^a$ | $4.964\pm1.21^b$ |
| 1:10 Potato | $3.412\pm0.87^a$ | $5.643\pm0.33^a$ | $1.417\pm0.08^a$ | $8.733\pm1.15^a$ |
| SEm. | 0.364 | 0.260 | 0.097 | 0.564 |
| CD | 1.259 | 0.900 | 0.336 | 1.952 |
| CV% | 27.96 | 10.23 | 15.14 | 16.92 |

Values are mean±S.D. Treatments with same letters are not significantly different ($P<0.05$)
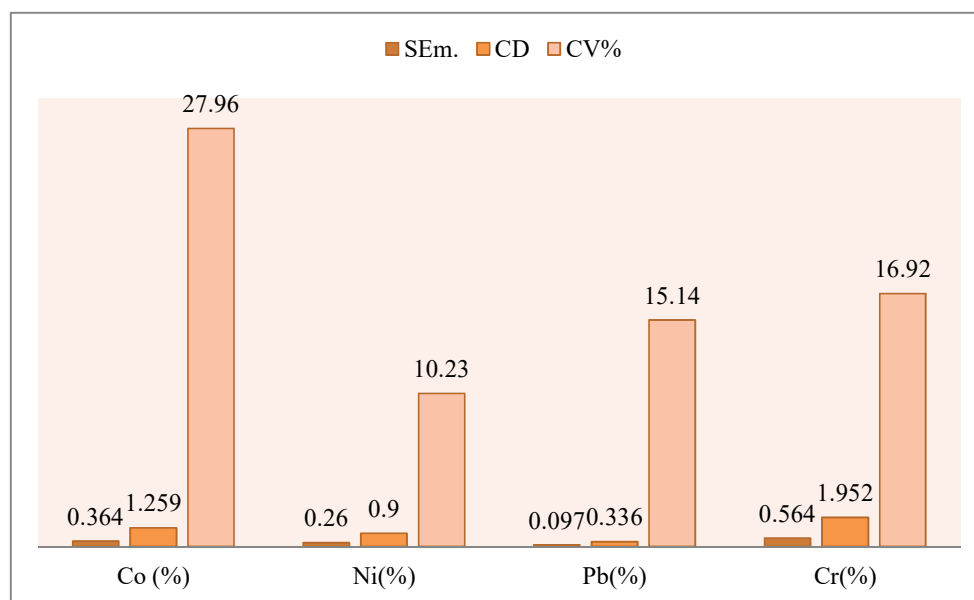


**Figure 12:** Elimination of high concentrations of toxic heavy metals

Table 3 presents the results of the study, which focus on the elimination of high concentrations of toxic heavy metals using various adsorbent doses in the form of SNPs in combination with potatoes. The data offers critical insights into the efficiency of these SNPs in removing specific toxic heavy metals, namely Co, Ni, Pb, and Cr. The results are presented in percentages, representing the reduction in metal content after a specified treatment. The table also includes standard error (SEm.), critical difference (CD), and coefficient of variation (CV%) values to provide statistical context for the findings. The outcomes demonstrate a

clear trend regarding the effectiveness of the SNPs in eliminating these toxic heavy metals. The table is divided into three columns, each indicating a different adsorbent dose or ratio of SNPs to potatoes. The results are presented for each of the four toxic heavy metals, allowing for a comprehensive assessment of their removal capabilities. In the 1:2 Potato ratios, it is observed that the SNPs were successful in reducing the content of Cobalt by 1.298% with a standard error of 0.62. For Ni, a reduction of 3.382% was achieved, with a standard error of 0.30. Likewise, Lead saw a reduction of 0.655% with a standard error of 0.22, and Chromium exhibited a reduction of 3.623% with a standard error of 0.25. These results, indicated by the letter "b," signify that there were no statistically significant differences among these values.

When the 1:5 Potato ratios was used, the efficacy of the SNPs in reducing toxic heavy metal content became more apparent. Cobalt displayed a reduction of 2.049% with a standard error of 0.28, while Ni exhibited a more substantial reduction of 4.182% with a standard error of 0.64. Lead showed a reduction of 1.264% with a standard error of 0.16, while Chromium underwent a 4.964% reduction with a standard error of 1.21. The notable point here is that for Lead, the value is marked with the letter "a," indicating a statistically significant difference compared to the 1:2 Potato ratios, whereas the other values are not significantly different ("b"). The most remarkable results are observed in the 1:10 Potato ratio, where the SNPs showcased their highest efficiency in heavy metal removal. Co experienced a substantial reduction of 3.412% with a standard error of 0.87, and Nickel displayed an even more impressive reduction of 5.643% with a standard error of 0.33. Lead exhibited a reduction of 1.417% with a standard error of 0.08, and Chromium showed the most substantial reduction of 8.733% with a standard error of 1.15. These results, indicated by the letter "a," signify statistically significant differences compared to both the 1:2 and 1:5 Potato ratios, underscoring the dose-dependent nature of heavy metal removal by SNPs.

The standard error (SEm.) values provide insights into the precision of the measurements, while the critical difference (CD) values help to identify statistically significant differences between treatments. The coefficient of variation (CV%) provides information on the variability of the data.

## 5.5: DISCUSSION

The study conducted a comprehensive analysis of the potential of SNPs synthesized from RHA as a biomass adsorbent for the removal of harmful heavy metals from potatoes. The

discussion of the study focuses on several key aspects of the research, including the characterization of SNPs, their effectiveness in heavy metal removal, and the implications of the findings.

The study utilized various characterization techniques to understand the structural and morphological properties of the synthesized SNPs. This included FT-IR analysis, SEM, EDX, DLS, TEM, AFM, and XRD. These characterizations provided valuable insights into the composition, size, shape, and distribution of the SNPs. Notably, the study found that the SNPs exhibited a well-dispersed particle size distribution, with sizes ranging from 20 to 50 nm. The characterization data indicated the potential of these SNPs for various applications, particularly in the field of environmental remediation. The study addressed the critical issue of heavy metal contamination in potatoes, focusing on a variety known as "Kufri Badshah." Heavy metals such as Co, Ni, Pb, and Cr can accumulate in plants, particularly potatoes, when they are grown in contaminated soil or water. The findings revealed that these heavy metals displayed different accumulation patterns in potato tubers, with Fe, Zn, Mn, Cu, Ni, Pb, and Cd showing variations in their concentrations. The study emphasized the importance of food safety and the need to monitor and quantify heavy metal concentrations in potatoes to safeguard consumer health.

One of the key aspects of the study was the investigation of how varying biomass concentrations (SNPs to Potato ratios) influenced the removal of heavy metals from potatoes. The data in Table 3 showed that the use of SNPs at different ratios effectively eliminated heavy metals, with substantial differences observed between the 1:2 and 1:10 ratios. The results indicated that the efficiency of SNPs in removing hazardous heavy metals from potatoes was not significantly affected by the quantity of potatoes present. This highlights the potential for scalable and efficient heavy metal remediation processes using SNPs. The findings of the study have significant implications for both environmental science and public health. The successful synthesis of SNPs from RHA offers an environmentally friendly and cost-effective approach to producing nanoparticle adsorbents. These SNPs demonstrated potential in removing harmful heavy metals, suggesting their utility in environmental and agricultural applications. The research also emphasized the importance of careful selection of adsorbent doses based on the target heavy metal and specific site conditions for optimal removal.

## 5.6: REFERENCES

[1] Manwani, Seema, C. R. Vanisree, Vibha Jaiman, Kumud Kant Awasthi, Chandra Shekhar Yadav, Mahipal Singh Sankhla, Pritam P. Pandit, and Garima Awasthi; "Heavy metal contamination in vegetables and their toxic effects on human health"; Sustainable Crop Production: Recent Advances; 181 (2022).

[2] Chen, Yongshan, Jinghua Xu, Zhengyong Lv, Liumei Huang, and Jinping Jiang; "Impacts of biochar and oyster shells waste on the immobilization of arsenic in highly contaminated soils."; Journal of environmental management; 217 (2018) 646-653.

[3] Järup, L; "Hazards of heavy metal contamination"; British Medical Bulletin; 68 (2003).

[4] İslamoğlu, Ayşe Hümeyra, Tuğba Kahvecioğlu, Gökçe Bönce, Esra Gedik, and Fatma GÜNEŞ. "Determination of heavy metals in some fruits, vegetables and fish by ICP-MS." Eurasian Journal of Food Science and Technology 5, no. 1 (2021): 67-76.

[5] Hossain, SK S., Lakshya Mathur, and P. K. Roy. "Rice husk/rice husk ash as an alternative source of silica in ceramics: A review." Journal of Asian Ceramic Societies 6, no. 4 (2018): 299-313.

[6] Goodman, Bernard A. "Utilization of waste straw and husks from rice production: A review." Journal of Bioresources and Bioproducts 5, no. 3 (2020): 143-162.

[7] FAO, FAOSTAT. "Food and agriculture organization of the United Nations." Rome, URL: http://faostat. fao. org (2018).

[8] Moraes, Carlos AM, Iara J. Fernandes, Daiane Calheiro, Amanda G. Kieling, Feliciane A. Brehm, Magali R. Rigon, Jorge A. Berwanger Filho, Ivo AH Schneider, and Eduardo Osorio. "Review of the rice production cycle: by-products and the main applications focusing on rice husk combustion and ash recycling." Waste Management & Research 32, no. 11 (2014): 1034-1048.

[9] Bodie, Aaron R., Andrew C. Micciche, Griffiths G. Atungulu, Michael J. Rothrock Jr, and Steven C. Ricke. "Current trends of rice milling byproducts for agricultural applications and alternative food production systems." Frontiers in Sustainable Food Systems 3 (2019): 47.

[10] Dhankhar, Poonam, and T. Hissar. "Rice milling." IOSR J. Eng 4, no. 5 (2014): 34-42.

[11] Dorairaj, Deivaseeno, Nisha Govender, Sarani Zakaria, and Ratnam Wickneswari. "Green synthesis and characterization of UKMRC-8 rice husk-derived mesoporous silica nanoparticle for agricultural application." Scientific Reports 12, no. 1 (2022): 20162.

[12] Sekhar, K. Chandra, C. T. Kamala, N. S. Chary, and Y. Anjaneyulu. "Removal of heavy metals using a plant biomass with reference to environmental control." International Journal of Mineral Processing 68, no. 1-4 (2003): 37-45.

[13] Okoronkwo, Elvis A., Patrick Ehi Imoisili, Smart A. Olubayode, and Samuel OO Olusunle. "Development of silica nanoparticle from corn cob ash." Advances in Nanoparticles 5, no. 02 (2016): 135-139.

[14] Chen, Jiucun, Mingzhu Liu, Chen Chen, Honghong Gong, and Chunmei Gao. "Synthesis and characterization of silica nanoparticles with well-defined thermoresponsive PNIPAM via a combination of RAFT and click chemistry." ACS applied materials & interfaces 3, no. 8 (2011): 3215-3223.

[15] Guo, Wenwen, Guoneng Li, Youqu Zheng, and Ke Li. "Nano-silica extracted from rice husk and its application in acetic acid steam reforming." RSC advances 11, no. 55 (2021): 34915-34922.

[16] Nayak, P. P., and A. K. Datta. "Synthesis of SiO2-nanoparticles from rice husk ash and its comparison with commercial amorphous silica through material characterization." Silicon 13, no. 4 (2021): 1209-1214.

[17] Vinoda, B. M., M. Vinuth, Y. D. Bodke, and J. Manjanna. "Photocatalytic degradation of toxic methyl red dye using silica nanoparticles synthesized from rice husk ash." J. Environ. Anal. Toxicol 5, no. 1000336 (2015): 2161-0525.

[18] Hu, Sixiao, and You-Lo Hsieh. "Preparation of activated carbon and silica particles from rice straw." ACS Sustainable Chemistry & Engineering 2, no. 4 (2014): 726-734.

[19] Helmiyati, H., and R. P. Suci. "Nanocomposite of cellulose-ZnO/SiO2 as catalyst biodiesel methyl ester from virgin coconut oil." In AIP conference proceedings, vol. 2168, no. 1. AIP Publishing, 2019.

[20] Zhang, Xiaotian, Yangyi Sun, Yijing Mao, Kunlin Chen, Zhihai Cao, and Dongming Qi. "Controllable synthesis of raspberry-like PS–SiO 2 nanocomposite particles via Pickering emulsion polymerization." RSC advances 8, no. 7 (2018): 3910-3918.

[21] Alhadhrami, A., Gehad G. Mohamed, Ahmed H. Sadek, Sameh H. Ismail, A. A. Ebnalwaled, and Abdulraheem SA Almalki. "Behavior of silica nanoparticles synthesized from rice husk ash by the sol–gel method as a photocatalytic and antibacterial agent." Materials 15, no. 22 (2022): 8211.

[22] Mohseni, Meysam, Kambiz Gilani, and Seyed Alireza Mortazavi. "Preparation and characterization of rifampin loaded mesoporous silica nanoparticles as a potential system for pulmonary drug delivery." Iranian journal of pharmaceutical research: IJPR 14, no. 1 (2015): 27.

[23] Zhao, Zongzhe, Chao Wu, Ying Zhao, Yanna Hao, Ying Liu, and Wenming Zhao. "Development of an oral push–pull osmotic pump of fenofibrate-loaded mesoporous silica nanoparticles." International Journal of Nanomedicine (2015): 1691-1701.

[24] Abduraimova, Aiganym, Anara Molkenova, Assem Duisembekova, Tomiris Mulikova, Damira Kanayeva, and Timur Sh Atabaev. "Cetyltrimethylammonium bromide (CTAB)-

loaded SiO2–Ag mesoporous nanocomposite as an efficient antibacterial agent." Nanomaterials 11, no. 2 (2021): 477.

[25] Dang, Nhung Thi Thuy, Trinh Thi Ai Nguyen, Tuan Dinh Phan, Hoa Tran, Phu Van Dang, and Hien Quoc Nguyen. "Synthesis of silica nanoparticles from rice husk ash." VNUHCM Journal of Science and Technology Development 20, no. K7 (2017): 50-54.

[26] Saha, Arighna, Kritika Narula, Prashant Mishra, Goutam Biswas, and Snehasis Bhakta. "A facile cost-effective electrolyte-assisted approach and comparative study towards the Greener synthesis of silica nanoparticles." Nanoscale Advances 5, no. 5 (2023): 1386-1396.

[27] Patil, Nita Babaso, H. Sharanagouda, S. R. Doddagoudar, C. T. Ramachandra, and K. T. Ramappa. "Biosynthesis and characterization of silica nanoparticles from rice (Oryza sativa L.) husk." Int. J. Curr. Microbiol. App. Sci 7, no. 12 (2018): 2298-2306.

[28] Brunauer, S., Emmett, P. H., & Teller, E. (1938). Adsorption of Gases in Multimolecular Layers. Journal of the American Chemical Society, 60(2), 309–319. https://doi.org/10.1021/ja01269a023.

[29] Sing, K. S. W. (1985). Reporting Physisorption Data for Gas/Solid Systems with Special Reference to the Determination of Surface Area and Porosity (Recommendations 1984). Pure and Applied Chemistry, 57(4), 603–619. https://doi.org/10.1351/pac198557040603.

[30] R. W., Giri, N., & Choudhary, M. (2017). Silica Nanoparticles Synthesis and Applications: A Review. Critical Reviews in Solid State and Materials Sciences, 42(3), 245–277. https://doi.org/10.1080/10408436.2016.1177960.

[31] Le, Van Hai, Chi Nhan Ha Thuc, and Huy Ha Thuc. "Synthesis of silica nanoparticles from Vietnamese rice husk by sol–gel method." Nanoscale research letters 8 (2013): 1-10.

[32] Rovani, Suzimara, Jonnatan J. Santos, Paola Corio, and Denise A. Fungaro. "Highly pure silica nanoparticles with high adsorption capacity obtained from sugarcane waste ash." ACS omega 3, no. 3 (2018): 2618-2627.

[33] Dung, Pham Dinh, Nguyen Ngoc Duy, Nguyen Ngoc Thuy, Lu T. Minh Truc, Bui Van Le, Dang Van Phu, and Nguyen Quoc Hien. "Effect of nanosilica from rice husk on the growth enhancement of chili plant (Capsicum frutescens L.)." Vietnam Journal of Science and Technology 54, no. 5 (2016): 607.

[34] Hung, Dao Phi, Nguyen Thien Vuong, Dang Manh Hieu, Nguyen Thi Linh, Trinh Van Thanh, Nguyen Anh Hiep, and Duong Manh Tien. "Effect of silica nanoparticles on properties of coatings based on acrylic emulsion resin." Vietnam Journal of Science and Technology 56, no. 3B (2018): 117-125.

[35] AbouAitah, K. E. A., A. A. Farghali, A. Swiderska-Sroda, W. Lojkowski, A. M. Razin, and M. K. Khedr. "Mesoporous silica materials in drug delivery system: pH/glutathione-responsive release of poorly water-soluble pro-drug quercetin from two and three-dimensional pore-structure nanoparticles." J. Nanomed. Nanotechnol 7, no. 02 (2016).

[36] Awizar, Denni Asra, Norinsan Kamil Othman, Azman Jalar, Abdul Razak Daud, I. Abdul Rahman, and N. H. Al-Hardan. "Nanosilicate extraction from rice husk ash as green corrosion inhibitor." International Journal of Electrochemical Science 8, no. 2 (2013): 1759-1769.

[37] abualnoun Ajeel, Sami, Khalid A. Sukkar, and Naser Korde Zedin. "Extraction of high purity amorphous silica from rice husk by chemical process." In IOP Conference Series: Materials Science and Engineering, vol. 881, no. 1, p. 012096. IOP Publishing, 2020.

[38] Kestens, Vikram, Gert Roebben, Jan Herrmann, Åsa Jämting, Victoria Coleman, Caterina Minelli, Charles Clifford et al. "Challenges in the size analysis of a silica nanoparticle mixture as candidate certified reference material." Journal of Nanoparticle Research 18 (2016): 1-22.

[39] Moosa, A. Ahmed, and Ban F. Saddam. "Synthesis and characterization of nanosilica from rice husk with applications to polymer composites." American Journal of Materials Science 7, no. 6 (2017): 223-231.

[40] Sharma, Sanjeev K., Gaurav Sharma, Abhishek Sharma, Kirti Bhardwaj, Km Preeti, K. Singh, Anirudh Kumar et al. "Synthesis of silica and carbon-based nanomaterials from rice husk ash by ambient fiery and furnace sweltering using a chemical method." Applied Surface Science Advances 8 (2022): 100225.

[41] Agi, Augustine, Radzuan Junin, Mohd Zaidi Jaafar, Rahmat Mohsin, Agus Arsad, Afeez Gbadamosi, Cheo Kiew Fung, and Jeffrey Gbonhinbor. "Synthesis and application of rice husk silica nanoparticles for chemical enhanced oil recovery." Journal of Materials Research and Technology 9, no. 6 (2020): 13054-13066.

[42] Knipping, Jörg, Hartmut Wiggers, Bernd Rellinghaus, Paul Roth, Denan Konjhodzic, and Cedrik Meier. "Synthesis of high purity silicon nanoparticles in a low pressure microwave reactor." Journal of nanoscience and nanotechnology 4, no. 8 (2004): 1039-1044.

[43] F Hincapié Rojas, Daniel, Posidia Pineda Gómez, and Andrés Rosales Rivera. "Production and characterization of silica nanoparticles from rice husk." Advanced Materials Letters 10, no. 1 (2019): 67-73.

[44] Atta, A. Y., B. Y. Jibril, B. O. Aderemi, and S. S. Adefila. "Preparation of analcime from local kaolin and rice husk ash." Applied Clay Science 61 (2012): 8-13.

[45] Vijayan, R., G. Suresh Kumar, Gopalu Karunakaran, N. Surumbarkuzhali, S. Prabhu, and R. Ramesh. "Microwave combustion synthesis of tin oxide-decorated silica nanostructure using rice husk template for supercapacitor applications." Journal of Materials Science: Materials in Electronics 31 (2020): 5738-5745.

[46] Alengebawy, Ahmed, Sara Taha Abdelkhalek, Sundas Rana Qureshi, and Man-Qun Wang. "Heavy metals and pesticides toxicity in agricultural soil and plants: Ecological risks and human health implications." Toxics 9, no. 3 (2021): 42.

[47] Tariq, Farah, Xiukang Wang, Muhammad Hamzah Saleem, Zafar Iqbal Khan, Kafeel Ahmad, Ifra Saleem Malik, Mudasra Munir et al. "Risk assessment of heavy metals in basmati rice: Implications for public health." Sustainability 13, no. 15 (2021): 8513.

[48] Morgan, Jeffrey N. "Effects of processing on heavy metal content of foods." Impact of processing on food safety (1999): 195-211.

[49] Hajeb, P., Jens Jørgen Sloth, S. H. Shakibazadeh, N. A. Mahyudin, and L. Afsah-Hejri. "Toxic elements in food: occurrence, binding, and reduction approaches." Comprehensive Reviews in Food Science and Food Safety 13, no. 4 (2014): 457-472.

[50] Hezbullah, M., S. Sultana, S. R. Chakraborty, and M. I. Patwary. "Heavy metal contamination of food in a developing country like Bangladesh: An emerging threat to food safety." Journal of Toxicology and Environmental Health Sciences 8, no. 1 (2016): 1-5.

[51] De Toni, Luca, Francesco Tisato, Roberta Seraglia, Marco Roverso, Valentina Gandin, Cristina Marzano, Roberto Padrini, and Carlo Foresta. "Phthalates and heavy metals as endocrine disruptors in food: a study on pre-packed coffee products." Toxicology reports 4 (2017): 234-239.

[52] Tajik, Sepideh, Parisa Ziarati, and L. Cruz-Rodriguez. "Coffee waste as novel bio-adsorbent: detoxification of nickel from contaminated soil and Coriandrum Sativum." methods 38, no. 41 (2020): 2693-2504.